SENSORS

Biomimetic temperature-sensing layer for artificial skins

Raffaele Di Giacomo,[1] Luca Bonanomi,[1,2] Vincenzo Costanza,[1,2] Bruno Maresca,[3] Chiara Daraio[2]*

Artificial membranes that are sensitive to temperature are needed in robotics to augment interactions with humans and the environment and in bioengineering to improve prosthetic limbs. Existing flexible sensors achieved sensitivities of <100 millikelvin and large responsivity, albeit within narrow (<5 kelvin) temperature ranges. Other flexible devices, working in wider temperature ranges, exhibit orders of magnitude poorer responses. However, much more versatile and temperature-sensitive membranes are present in animals such as pit vipers, whose pit membranes have the highest sensitivity and responsivity in nature and are used to locate warm-blooded prey at distance. We show that pectin films mimic the sensing mechanism of pit membranes and parallel their record performances. These films map temperature on surfaces with a sensitivity of at least 10 millikelvin in a wide temperature range (45 kelvin), have very high responsivity, and detect warm bodies at distance. The produced material can be integrated as a layer in artificial skin platforms and boost their temperature sensitivity to reach the best biological performance.

INTRODUCTION

Artificial skins (*1*, *2*) are essential to augment robotics (*3*) and improve prosthetic limbs (*4*). Existing platforms are designed to emulate properties of the human skin by incorporating sensitive functions (*4*–*8*) that respond to different external stimuli, for example, to variations of temperature (*4*, *8*–*10*). Available artificial skins that sense temperature variations use either passive flexible resistors (*8*–*11*) or active electronic devices (*4*, *12*). Their functionality is limited by the choice of temperature-sensitive materials incorporated in the electronics (*2*). For example, p-n junctions have small responsivity, require a complex architecture, and demand nontrivial fabrication procedures (*4*, *12*). Flexible sensors made of monolayer-capped nanoparticles are, at the same time, as sensitive to temperature as they are to pressure and humidity, making it impossible to deconvolve the three variables in practical applications (*8*). Composites based on a polymer matrix and electrically conductive fillers operate in a too narrow temperature range and have two orders of magnitude uncertainty on the current value corresponding to the same temperature (*9*, *13*). Substantial advances on artificial skins require the use of new flexible materials with higher temperature sensitivity, responsivity, range of operation, and stability.

Recently, it has been shown that materials composed of plant cells and carbon nanotubes have very high responsivity over large temperature ranges (*14*). However, these materials are not suitable for artificial skins because they have mechanical properties similar to wood, are not flexible, and require cumbersome fabrication approaches. Here, we focus on the active molecule responsible for the large temperature responsivity in plant cells (pectin) (*14*) and engineer films suitable for flexible electronic devices.

Pectin, a component of all higher plant cell walls, is made of very structurally and functionally complex, acid-rich polysaccharides (*15*). Pectin plays several roles in plants; for example, it is an essential structural component of cell walls that binds ions and enzymes (*16*). In high-ester pectins, at acidic pH, individual chains are linked together by hydrogen bonds and hydrophobic interactions. In contrast, in low-ester pectins, ionic bridges are formed, at near neutral pH, between Ca^{2+} ions and the ionized carboxyl groups of the galacturonic acid, forming an "egg box" in which cations are stored (*17*). Because the cross-linkings between pectin molecules decrease exponentially with temperature (*18*), increasing the temperature of a Ca^{2+}–cross-linked pectin increases ionic conduction (*14*).

RESULTS

We produced pectin films and compared their temperature responsivity (i.e., the signal variation in a given temperature increment) with the best flexible temperature-sensing films (*4*, *8*, *10*) in a biologically relevant temperature interval of 45 K (Fig. 1A). The pectin film (Fig. 1B) signal variation is about two orders of magnitude greater than the others (*4*, *8*, *10*). A higher responsivity has been reported only for a very narrow temperature range (<5 K) for a two-state device (i.e., a temperature switch) (*9*).

To find a closer match to the pectin film's responsivity, sensitivity, and range of operation, it must be compared directly with biological membranes. Human skin, for example, senses temperature with a sensitivity of 20 mK (*19*) through ion channels (*20*) that belong to the family of the transient receptor potential (TRP) sensors and include the snake TRPA1 ortholog (*20*), which is the most sensitive temperature sensor in nature. Snakes are cold-blooded animals, and their body temperature corresponds to that of the environment. Snakes' pit membranes (*21*) distinguish minute temperature variations. The extraordinary sensitivity of pit membranes is due to the presence of voltage-gated ion channel orthologs of the wasabi receptor (*21*) in humans. At night, thermal emission from a mammalian prey at a maximum distance of 1 m away causes a small, local temperature increase on the membranes (*21*). The small temperature increase leads to an increased opening of TRPA1 ion channels (*20*–*22*) and to an increased current carried by Ca^{2+} ions (Fig. 1C) (*21*) through the cell membrane. The mechanism of detection (*23*) of the pit membrane is not photochemical because the incident thermal radiation is not converted directly into electrical current (*21*). For this reason, the pit membrane response to temperature has been characterized, measuring the current variation when placed in contact with a warm surface, that is, as a thermometer film rather than an optical receiver in the far-infrared range (*21*). At the time of publication, we know of no

[1]Department of Mechanical and Process Engineering (D-MAVT), Swiss Federal Institute of Technology (ETH), Zurich, Switzerland. [2]Division of Engineering and Applied Science, California Institute of Technology, Pasadena, CA 91125, USA. [3]Department of Pharmacy, Division of Biomedicine, University of Salerno, Fisciano, Italy.
*Corresponding author. Email: daraio@caltech.edu

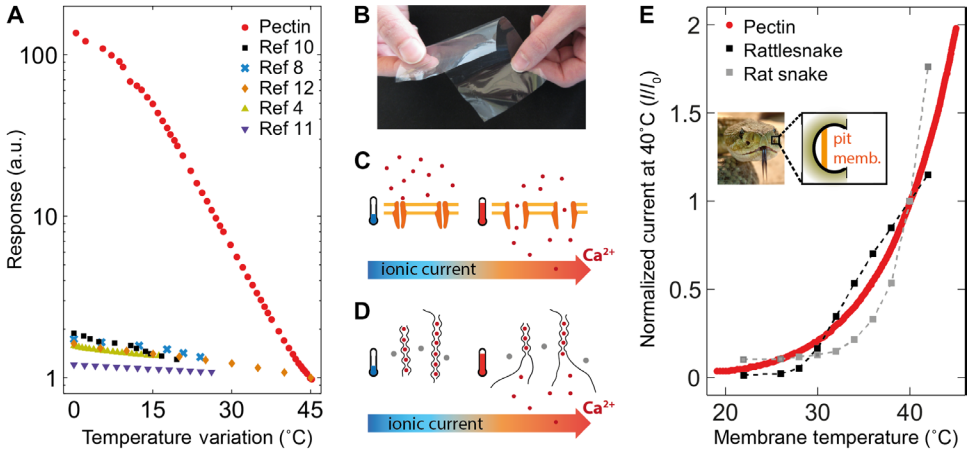

Fig. 1. Comparison between artificial skins, snakes' pit membrane, and pectin films. (**A**) Responses of different artificial skins to temperature. Normalized signal variation as a function of relative temperature change. Red dots, pectin film resistance; black squares, resistance replotted from Park *et al.* (*10*); blue crosses, resistance replotted from Segev-Bar *et al.* (*8*); orange diamonds, resistance replotted from Trung *et al.* (*12*); green triangles, voltage replotted from Kim *et al.* (*4*); violet triangles, resistance replotted from Webb *et al.* (*11*). a.u., arbitrary units. (**B**) A sample of the produced pectin films showing its flexibility. (**C**) Molecular mechanism governing pit membrane sensitivity. Dark orange, TRPA1 channels; light orange, cell membrane; red dots, Ca^{2+} ions. (**D**) Molecular mechanism governing cross-linked pectin films' sensitivity. Black lines, galacturonic acid; red dots, Ca^{2+} ions; gray dots, water molecules. (**E**) Comparison with pit membranes. Red dots, normalized current in a pectin film. The points with error bars and dotted lines are plotted from Gracheva *et al.* (*21*). Dark gray dots, rattle snake; light gray dots, rat snake. Inset: Image of a rattlesnake (left) and schematic of the pit organ and pit membrane (right).

engineered material with similar thermal sensitivity or responsivity in a comparable range of temperatures. Here, we show that pectin films mimic the mechanism of the TRP receptors by using a similar Ca^{2+} current regulation (Fig. 1D) and achieve the same sensing performance of snakes' pit membranes (Fig. 1E).

We fabricated films (~200 μm thick) by casting a pectin solution in a mold (see Materials and Methods); thinner films can be produced by spin coating. The pectin was cross-linked in a $CaCl_2$ solution and dehydrated in vacuum to obtain a transparent film. After dehydration, the conductivity of the hydrogel is in the order of 0.1 mS m^{-1}. The current-voltage characteristic of a typical film is linear (fig. S1). To characterize the response of the material to temperature, we measured the samples' current between 10° and 55°C on a Peltier element. The temperature was monitored with an independent calibrated Pt100 sensor. The thermal responsivity achieved was comparable with that of rat and rattle snakes' pit membranes (Fig. 1E). The responsivity was also within the same order of magnitude of the plant cell–carbon nanotube composites (*14*). However, the produced pectin films are transparent, flexible, and conformable to any surface; thus, they are ideal as sensitive layer in synthetic skins.

To prove their sensing mechanism, we made three control experiments measuring the temperature responsivity of (i) pure water, (ii) pectin films with pure water and no cross-linking ions, and (iii) a $CaCl_2$ solution. The temperature response in the three cases was much lower than that of the Ca^{2+}–cross-linked pectin (see fig. S2). This result indicates that the large responsivity of the cross-linked pectin films is due to interactions between pectin chains and the Ca^{2+} ions, as shown in Fig. 1D and reported in (*14*). To measure the stability of the Ca^{2+}–cross-linked pectin films, we cycled them in an interval of 30 K (Fig. 2A). The films are very stable over the 215 cycles tested (Fig. 2A), showing no significant change of responsivity (Fig. 2B) or of absolute current values at each temperature (Fig. 2C). The activation energy for pectin films is 81.9 kJ mol^{-1} (see fig. S3, A and B, and the Supplementary Materials). A similar value of the pectin activation energy was reported in rheological measurements (*18*).

We tested the sensitivity of the pectin films, monitoring the local temperature of a sample (Fig. 2D) with a thermal camera while an independent source meter measured its electrical current. The film responds with fidelity to small changes of the environmental temperature (Fig. 2, D and E). The detailed data for a 2-s time interval (Fig. 2E) reveal that the film senses temperature variations of at least 10 mK. To compare the performance of our material with that of the viper's pit membrane, we characterized the sensitivity of pectin films when facing small, warm bodies at a distance. A microwavable stuffed animal was heated up to 37°C. A thermal camera was used to determine its temperature and ensure that it remained constant during the measurements. We placed the teddy bear 1 m from the membrane for ~20 s and then removed it. We repeated this procedure also at distances of 0.6 and 0.4 m. The results show that the membrane detects warm bodies, about the size of a rat or a small rabbit, at a distance of 1 m (Fig. 2F).

We also performed experiments with larger films (21 cm × 29.7 cm) connected to two carbon electrodes and operating at 20 V (see Materials and Methods, and movie S1). These samples have the same sensitivity, as measured in smaller films (Fig. 1E). To test the response of the films to bending, we monitored their current at constant temperature in different bending positions (Fig. 3A and fig. S4). The current variations due to bending are negligible compared with the variations induced by small temperature changes (Fig. 3A). We also tested the response of a bent sample to temperature variations (Fig. 3B) and found no change in responsivity. The experiments in Fig. 3B were performed on a copper bent substrate covered with an insulation layer.

To verify that pectin films can be integrated in a synthetic skin as a temperature-sensitive material, we fabricated samples (52 mm × 52 mm) with multiple electrodes (8 or 16 contacts) deposited on the external frame (fig. S5, A and B). These samples were made of pectin films, with chromium/gold electrical contacts sandwiched between two insulating layers to protect them from the effect of direct contact with external conductors and/or humidity/water (Fig. 3C). We monitored the signal between electrodes of each row and column while increasing the temperature in selected areas of the skins. On the basis of the number of contacts on the outer frame, we divided the area of the sample into 4 (or 16) blocks, corresponding to the number of "pixels." Each pixel is addressed as the intersection between each row and column, according to the electrodes' position. This arrangement allowed us to reconstruct the temperature map on the material without cumbersome or pixel-addressed electronics (*3*, *9*). Mapping of complex temperature profiles can be further enhanced by algorithmic analysis (*24*, *25*).

The measurements obtained from the 4-pixel sample were performed using the circuit shown in fig. S6 operating at 18 V and explained in the Supplementary Materials. The position of a finger touching four

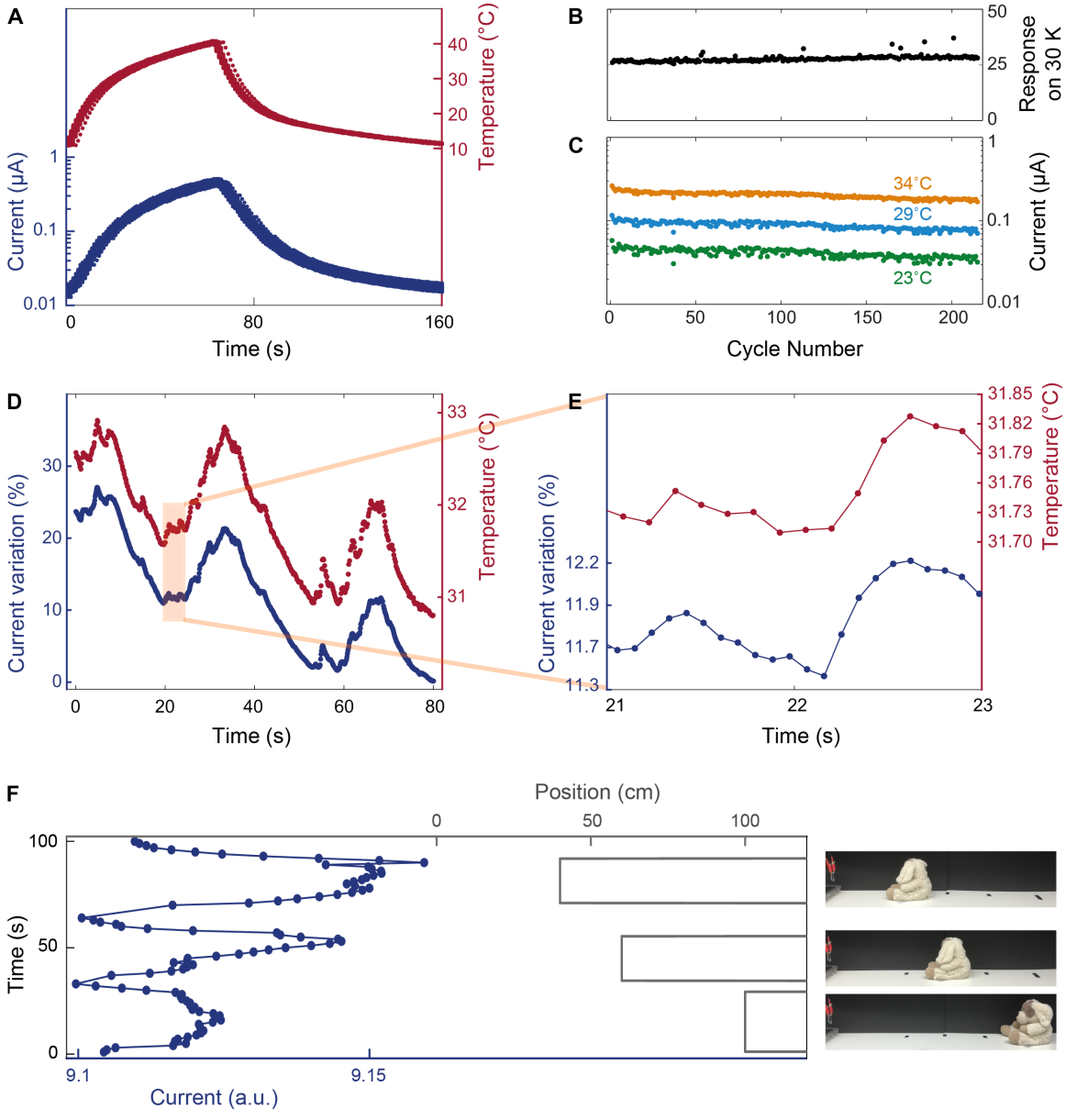

Fig. 2. Characterization of the pectin films. (**A**) Red dots, forced temperature, 215 cycles superimposed; blue dots, corresponding electrical current in a pectin film, 215 cycles superimposed. (**B**) Responsivity: Electrical current ratio between 40° and 10°C during the 215 cycles displayed in (A). (**C**) Electrical current in the pectin film at different temperatures during the 215 cycles displayed in (A). (**D**) Electrical current value in the pectin film (blue dots, left axis) plotted as a function of time and compared with the sample's temperature measured by the thermal camera (red dots, right axis). The temperature oscillations are caused by variations of the ambient temperature during the measurements. (**E**) Magnification of the data in the orange box in (D); dots, measurement points; lines are included as a guiding reference. (**F**) Sensing heat from a warm object (37°C) at a distance. Blue dots, electrical current in the pectin film; blue line is included as a guiding reference. Black line, position of the object with respect to the membrane positioned in 0.

different pixels of a skin for ~2 s is distinguishable from the electrical response of the materials (Fig. 3D). The voltage signals acquired are reported in Fig. 3D, fig. S7, and table S1. The noise in fig. S7 derives from the electronic readout circuit and not from the sensor, as confirmed by performing similar measurements with a pico-amperometer (fig. S8). The temperature variation on each pixel was ~1 K, as shown in the thermal image in fig. S9. To exclude piezoresistive effects, we performed the same measurements by pressing the sample with a metal object at the same temperature of the pixel (fig. S10). To test the response of pectin skins to an increased sensing spatial density, we fabricated a 16-pixel device in the same skin area and evaluated its temperature-mapping ability. We placed an aluminum parallelepiped (12 mm × 12 mm × 3mm) near the lower right corner of the skin at 26°C (with an ambient temperature of 20°C). As shown in Fig. 3E, we measured the signal on the skin for each of the 16 pixels 0.8 s after the aluminum square was laid in contact (table S2). The thermal camera map (fig. S11 and pixelated in Fig. 3F) and the temperature map obtained with our skin show an excellent match.

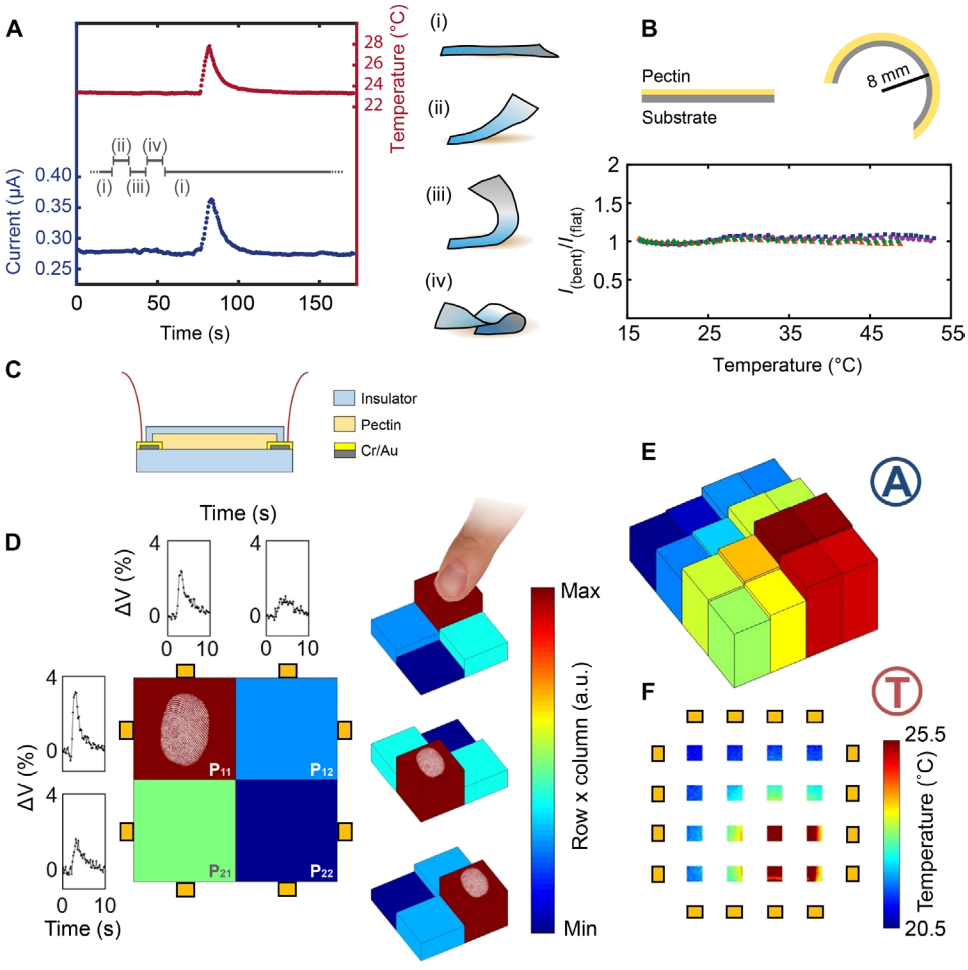

Fig. 3. Characterization of the pectin films as materials for artificial skins. (**A**) Current and temperature as a function of time while bending. At $t = 75$ s, the temperature was increased and then decreased by ~4 K. Right: Cartoons of the bending positions tested (see fig. S4 for images). (**B**) Current response when the sample is bent. Cartoon of the bending position of the film on a copper/insulator substrate. (**C**) Schematic view of the pectin skins in cross section. (**D**) Electrical response and temperature maps obtained with a 4-pixel skin when a finger touched it in different positions (refer to the fingerprint location in each panel). The voltage-time panels show the signal readout for the corresponding rows and columns. The colors (and heights of the blocks) correspond to the product between the maximum signal variations (in %) detected in each row and column (see the Supplementary Materials and table S1), normalized to 1. Figure S7 shows the percentage increase of the signal in time for each of the 4 pixels when individually touched. (**E**) Electrical response of a 16-pixel skin when a warm object is placed on its bottom right corner. (**F**) Pixelated thermal camera image of the skin corresponding to (E).

CONCLUSIONS

The present work demonstrates that a material composed exclusively of purified plant pectin and cross-linking ions, engineered into a film, has a performance equivalent to that of the snake's pit membrane and is superior to other flexible materials. The pectin films are ultralow-cost and scalable, are insensitive to pressure and bending, and can be used to augment temperature sensing when integrated in synthetic skin platforms.

The exquisite temperature sensitivity and mapping ability of pectin skins reveal opportunities in robotic sensing and haptics, where biomimetic sensors are important (*2*). For example, pectin skins could be embodied in robotic prosthetics, which are limited today by the need of improved sensory feedback (*26*). Feedback from prosthetics is essential to restore the complete functionality of a limb and is especially critical for achieving proper control of robotic devices, attaining much better results than with the single use of vision (*27*). Pectin skins can be used as a high-performance layer in flexible electronic devices, for example, when sandwiched in the architecture of an artificial skin or a prosthetic limb.

The record-high sensitivity of pectin skins makes them suitable to record finely distributed temperature maps on surfaces. Their ease of fabrication and minimal requirements for electronic circuitry make them compatible with most existing flexible technologies. Some limitations arise from the need of an insulating layer against excessive humidity. The insertion of a polymeric insulation layer in synthetic skins is a common practice and can offer a direct solution to the problem. Another limitation is the need for accurate initial calibration. Improving the uniformity of the pectin layers is expected to reduce the current calibration complexity.

MATERIALS AND METHODS

Pectin

Galacturonic acid comprises about 70% of pectin, and all pectic polysaccharides contain galacturonic acid linked at the O-1 and O-4 positions. Studies based on pectin biosynthesis have shown that pectin is synthesized in the Golgi apparatus and transported to the cell wall inside membrane vesicles (*28*). Once synthesized, polymers move to the cell wall by the movement of Golgi vesicles, possibly along actin filaments through their myosin motors (*28*). The observed heterogeneity in the pectin structure is due to species-, cell type–, and developmental state–specific differences in enzyme composition (*29*). Essentially, all studies on pectins have been performed on economically important plants, such as apple, citrus, sugar beet, and tomato, or on cultured cells, such as sycamore, carrot, spinach, and rose. Thus, very little is known of the 235,000 remaining known flowering plants and of pectins of green algae, liverworts, mosses, and ferns. In addition, characterization of pectin from cell wall mutants (*30*, *31*) and from plants growing in extreme environments may reveal unknown pectin structures with different properties. This variety suggests the large potential of pectin in future studies and synthesis of temperature-sensitive layers. Pectin biosynthesis probably requires at least 67 transferases (glycosyltransferase, methyltransferase, and acetyltransferase). It includes homogalacturonan, rhamnogalacturonan I, and the substituted galacturonans rhamnogalacturonan II and xylogalacturonan (*32*). In low-ester pectins, the gelation that occurs within the egg box is due

to the presence of calcium ions, which can be quickly reversed by monovalent sodium and potassium cations (*33*). An initial dimerization step of two homogalacturonic chains by cooperative bridging through Ca^{2+} ions determines the binding of the first calcium cation to two pectin chains, facilitating their alignment with respect to each other and allowing an easier binding of an upcoming calcium ion (*34*).

Film

To produce the materials, we used commercially available citrus low-methoxylated pectin with a degree of methylation of 34% and a content of galacturonic acid of 84% (Herbstreith & Fox). Pectin powder (2%, w/v) was dissolved at 80°C in deionized water and stirred at 1400 rpm until a uniform solution was obtained. To jellify the films, we prepared a 32 mM $CaCl_2$ solution (corresponding to a stoichiometric ratio $R = [Ca^{2+}]/2[COO^-] = 1$). The pectin solution was poured into a mold, and the $CaCl_2$ solution was then added. After gelation, the highly hydrated films were transferred to a vacuum chamber and dehydrated at 12 mbar overnight. Samples were then detached from the petri dish using a razor blade. The large samples shown in movie S1 were produced by pouring the gel on a glass substrate (28 cm × 30 cm × 0.5 cm) as the lower insulating layer. The electrical contacts were made of carbon tape, and a clear insulating acetate sheet (A4 paper format) was layered on top. To produce the skins, we deposited the pectin solution directly on different substrates [polydimethylsiloxane (PDMS), cellophane, or SiO_2], with predeposited electrical contacts made by sputtering chromium/gold or using carbon tape.

Polymeric insulation

We used polymeric insulation layers such as acetate (polyvinyl acetate) to protect the sensing layer from humidity and pH variations. This is a common practice in artificial skins. No chemical interaction between pectin and polyvinyl acetate or PDMS is expected because of their stable polymerized state. No change in responsivity or sensitivity was found with respect to pectin films without insulating layer when acetate or PDMS was used. Any other insulating material already in use for synthetic skins would serve for the scope.

Measurements

The electrical measurements reported in Figs. 1, 2, and 3 (A and B) and figs. S1 to S3, S8, and S10 were performed in a two-point contact geometry using a source measurement unit (Keithley model 2635), also referred to as amperometer or pico-amperometer. The electrical measurements in fig. S12 were acquired with a lock-in amplifier (model SR830, Stanford Research Systems). In the experiments described in Figs. 1 and 2, a dc polarizing voltage of 20 V was applied to the samples, and the current was allowed to decrease for ~2 hours. After the initial discharge, the current remained stable for several hours (during which experiments were performed). For the experiments in Fig. 3 (D and E), the applied voltage was a square wave with an amplitude of 18 V and a frequency of 5 Hz. Sampling rate was 10 samples per second. Temperature on the film was actuated by Peltier-Element Qc-31-1.4-8.5M. Independent temperature measurements on the film were measured with a Pt100 platinum thermometer. We also performed measurements at different frequencies (see fig. S12) up to 50°C. We found no difference in the temperature response of the pectin films under ac or dc conditions (see fig. S12). For the electrical measurements reported in Fig. 3 (D and E) and fig. S7, we sequentially applied the square wave voltage V to the electrical contacts in each row and column. We measured the signal output with the readout circuit (in fig. S6) connected to a data acquisition board (National Instruments BNC-2110). The thermal camera used in the experiments was FLIR A655sc.

Sensor's response and comparison

The metrological quantity of choice for the comparison in Fig. 1A is the response/responsivity defined as the amount of change in the output (readout signal) for a given change in the input (in this case, temperature). The scale in the plot is the same for all the sensors. Each value on the plot can be calculated as $(Output_{T2})/(Output_{T1})$ for each T2-T1 and with T1 fixed. The values were taken from the references cited, as reported in the legends and in the captions. Because the plot is in logarithmic scale, any arbitrary scaling factor will result in a translation of the curves up or down along the *y* axis, but the slope of the curves (response) will be preserved.

SUPPLEMENTARY MATERIALS

robotics.sciencemag.org/cgi/content/full/2/3/eaai9251/DC1

Methods

Fig. S1. Pectin film.

Fig. S2. Conductivity variation as a function of temperature in control experiments.

Fig. S3. Current-temperature characteristics of a pectin film and corresponding Arrhenius plot.

Fig. S4. Bending positions corresponding to experiment in Fig.3A.

Fig. S5. Setup for the electrical measurements performed on skins.

Fig. S6. Readout circuit for the 4-pixel skin.

Fig. S7. Voltage at the readout circuit for every row and column in a 4-pixel skin.

Fig. S8. Current versus time when the film is touched with a finger.

Fig. S9. Thermal image of the skin just after being touched with a finger.

Fig. S10. Effect of pressure and temperature on a 4-pixel skin.

Fig. S11. Aluminum square in contact with the 16-pixel skin.

Fig. S12. Alternating current measurements on the pectin films.

Table S1. Values corresponding to the block diagrams, with color map shown in Fig.3D.

Table S2. Values corresponding to the block diagram, with color map shown in Fig.3E.

Movie S1. Large-area film testing.

REFERENCES AND NOTES

1. J.-Y. Sun, C. Keplinger, G. M. Whitesides, Z. Suo, Ionic skin. *Adv. Mater.* **26**, 7608–7614 (2014).
2. A. Chortos, J. Liu, Z. Bao, Pursuing prosthetic electronic skin. *Nat. Mater.* **15**, 937–950 (2016).
3. M. Kaltenbrunner, T. Sekitani, J. Reeder, T. Yokota, K. Kuribara, T. Tokuhara, M. Drack, R. Schwödiauer, I. Graz, S. Bauer-Gogonea, S. Bauer, T. Someya, An ultra-lightweight design for imperceptible plastic electronics. *Nature* **499**, 458–463 (2013).
4. J. Kim, M. Lee, H. J. Shim, R. Ghaffari, H. R. Cho, D. Son, Y. H. Jung, M. Soh, C. Choi, S. Jung, K. Chu, D. Jeon, S.-T. Lee, J. H. Kim, S. H. Choi, T. Hyeon, D.-H. Kim, Stretchable silicon nanoribbon electronics for skin prosthesis. *Nat. Commun.* **5**, 5747 (2014).
5. B. C.-K. Tee, C. Wang, R. Allen, Z. Bao, An electrically and mechanically self-healing composite with pressure- and flexion-sensitive properties for electronic skin applications. *Nat. Nanotechnol.* **7**, 825–832 (2012).
6. B. Nie, R. Li, J. Cao, J. D. Brandt, T. Pan, Flexible transparent iontronic film for interfacial capacitive pressure sensing. *Adv. Mater.* **27**, 6055–6062 (2015).
7. B. C.-K. Tee, A. Chortos, A. Berndt, A. K. Nguyen, A. Tom, A. McGuire, Z. C. Lin, K. Tien, W.-G. Bae, H. Wang, P. Mei, H.-H. Chou, B. Cui, K. Deisseroth, T. N. Ng, Z. Bao, A skin-inspired organic digital mechanoreceptor. *Science* **350**, 313–316 (2015).
8. M. Segev-Bar, A. Landman, M. Nir-Shapira, G. Shuster, H. Haick, Tunable touch sensor and combined sensing platform: Toward nanoparticle-based electronic skin. *ACS Appl. Mater. Interfaces* **5**, 5531–5541 (2013).
9. T. Yokota, Y. Inoue, Y. Terakawa, J. Reeder, M. Kaltenbrunner, T. Ware, K. Yang, K. Mabuchi, T. Murakawa, M. Sekino, W. Voit, T. Sekitani, T. Someya, Ultraflexible, large-area, physiological temperature sensors for multipoint measurements. *Proc. Natl. Acad. Sci. U.S.A.* **112**, 14533–14538 (2015).
10. J. Park, M. Kim, Y. Lee, H. S. Lee, H. Ko, Fingertip skin–inspired microstructured ferroelectric skins discriminate static/dynamic pressure and temperature stimuli. *Sci. Adv.* **1**, e1500661 (2015).

11. R. C. Webb, A. P. Bonifas, A. Behnaz, Y. Zhang, K. J. Yu, H. Cheng, M. Shi, Z. Bian, Z. Liu, Y.-S. Kim, W.-H. Yeo, J. S. Park, J. Song, Y. Li, Y. Huang, A. M. Gorbach, J. A. Rogers, Ultrathin conformal devices for precise and continuous thermal characterization of human skin. *Nat. Mater.* **12**, 938–944 (2013).
12. T. Q. Trung, S. Ramasundaram, B.-U. Hwang, N.-E. Lee, An all-elastomeric transparent and stretchable temperature sensor for body-attachable wearable electronics. *Adv. Mater.* **28**, 502–509 (2016).
13. J. Jeon, H.-B.-R. Lee, Z. Bao, Flexible wireless temperature sensors based on Ni microparticle-filled binary polymer composites. *Adv. Mater.* **25**, 850–855 (2013).
14. R. Di Giacomo, C. Daraio, B. Maresca, Plant nanobionic materials with a giant temperature response mediated by pectin-Ca^{2+}. *Proc. Natl. Acad. Sci. U.S.A.* **112**, 4541–4545 (2015).
15. P. Sriamornsak, Chemistry of pectin and its pharmaceutical uses: A review. *Silpakorn Univ. J. Soc. Sci. Humanit. Arts* **3**, 206–228 (2003).
16. W. G. T. Willats, L. McCartney, W. Mackie, J. P. Knox, Pectin: Cell biology and prospects for functional analysis. *Plant Mol. Biol.* **47**, 9–27 (2001).
17. W. Plazinski, Molecular basis of calcium binding by polyguluronate chains. Revising the egg-box model. *J. Comput. Chem.* **32**, 2988–2995 (2011).
18. S. M. Cardoso, M. A. Coimbra, J. A. L. da Silva, Temperature dependence of the formation and melting of pectin–Ca^{2+} networks: A rheological study. *Food Hydrocoll.* **17**, 801–807 (2003).
19. R. W. Dykes, Coding of steady and transient temperatures by cutaneous "cold" fibers serving the hand of monkeys. *Brain Res.* **98**, 485–500 (1975).
20. L. Vay, C. Gu, P. A. McNaughton, The thermo-TRP ion channel family: Properties and therapeutic implications. *Br. J. Pharmacol.* **165**, 787–801 (2012).
21. E. O. Gracheva, N. T. Ingolia, Y. M. Kelly, J. F. Cordero-Morales, G. Hollopeter, A. T. Chesler, E. E. Sánchez, J. C. Perez, J. S. Weissman, D. Julius, Molecular basis of infrared detection by snakes. *Nature* **464**, 1006–1011 (2010).
22. C. E. Paulsen, J.-P. Armache, Y. Gao, Y. Cheng, D. Julius, Structure of the TRPA1 ion channel suggests regulatory mechanisms. *Nature* **520**, 511–517 (2015).
23. G. S. Bakken, A. R. Krochmal, The imaging properties and sensitivity of the facial pits of pitvipers as determined by optical and heat-transfer analysis. *J. Exp. Biol.* **210**, 2801–2810 (2007).
24. A. Borsic, R. Halter, Y. Wan, A. Hartov, K. D. Paulsen, Electrical impedance tomography reconstruction for three-dimensional imaging of the prostate. *Physiol. Meas.* **31**, S1–S16 (2010).
25. E. Santos, F. Simini, Comparison of electrical impedance tomography reconstruction techniques applied to IMPETOM system, in *13th IEEE International Conference on BioInformatics and BioEngineering* (Institute of Electrical and Electronics Engineers, 2013), pp. 1–4.
26. C. Antfolk, M. D'Alonzo, B. Rosén, G. Lundborg, F. Sebelius, C. Cipriani, Sensory feedback in upper limb prosthetics. *Expert Rev. Med. Devices* **10**, 45–54 (2013).
27. B. T. Nghiem, I. C. Sando, R. B. Gillespie, B. L. McLaughlin, G. J. Gerling, N. B. Langhals, M. G. Urbanchek, P. S. Cederna, Providing a sense of touch to prosthetic hands. *Plast. Reconstr. Surg.* **135**, 1652–1663 (2015).
28. A. Nebenführ, L. A. Gallagher, T. G. Dunahay, J. A. Frohlick, A. M. Mazurkiewicz, J. B. Meehl, L. A. Staehelin, Stop-and-go movements of plant Golgi stacks are mediated by the acto-myosin system. *Plant Physiol.* **121**, 1127–1142 (1999).
29. M. A. O'Neill, T. Ishii, P. Albersheim, A. G. Darvill, Rhamnogalacturonan II: Structure and function of a borate cross-linked cell wall pectic polysaccharide. *Annu. Rev. Plant Biol.* **55**, 109–139 (2004).
30. E. G. Burget, W.-D. Reiter, The *mur4* mutant of Arabidopsis is partially defective in the de novo synthesis of uridine diphospho L-arabinose. *Plant Physiol.* **121**, 383–389 (1999).
31. W.-D. Reiter, C. Chapple, C. R. Somerville, Mutants of *Arabidopsis thaliana* with altered cell wall polysaccharide composition. *Plant J.* **12**, 335–345 (1997).
32. D. Mohnen, Pectin structure and biosynthesis. *Curr. Opin. Plant Biol.* **11**, 266–277 (2008).
33. F. Munarin, M. C. Tanzi, P. Petrini, Advances in biomedical applications of pectin gels. *Int. J. Biol. Macromol.* **51**, 681–689 (2012).
34. C. M. G. C. Renard, M. C. Jarvis, Acetylation and methylation of homogalacturonans 1: Optimisation of the reaction and characterisation of the products. *Carbohydr. Polym.* **39**, 201–207 (1999).

Acknowledgments: We thank U. Marti (ETH Zurich) for the technical support and useful discussions. **Funding:** This work was supported by the Swiss National Science Foundation (grant 157162). **Author contributions:** R.D.G., L.B., V.C., B.M., and C.D. conceived the system and designed the research. R.D.G., L.B., and V.C. designed and performed the experiments. R.D.G. and V.C. designed the readout circuit for the electrical measurements. All authors contributed to the analysis of the data and discussions. L.B. and V.C. prepared the figures. R.D.G., V.C., L.B., and C.D. designed the supplementary movie. L.B. edited the movie. R.D.G. and C.D. wrote the manuscript. **Competing interests:** R.D.G., B.M., C.D., L.B., and V.C. are inventors on patent applications EP15161042.5, EP15195729.7, and PCT/EP2016/056642 that cover gel-based thermal sensors.

Submitted 31 August 2016
Accepted 28 December 2016
Published 1 February 2017
10.1126/scirobotics.aai9251

Citation: R. Di Giacomo, L. Bonanomi, V. Costanza, B. Maresca, C. Daraio, Biomimetic temperature-sensing layer for artificial skins. *Sci. Robot.* **2**, eaai9251 (2017).

Science Robotics

Biomimetic temperature-sensing layer for artificial skins

Raffaele Di Giacomo, Luca Bonanomi, Vincenzo Costanza, Bruno Maresca, and Chiara Daraio

Sci. Robot. **2** (3), eaai9251. DOI: 10.1126/scirobotics.aai9251

Science Robotics (ISSN 2470-9476) is published by the American Association for the Advancement of Science. 1200 New York Avenue NW, Washington, DC 20005. The title *Science Robotics* is a registered trademark of AAAS.